MOTION COMPENSATION IN STRIPMAP SAS SYSTEMS

MARCIN SZCZEGIELNIAK

University of Technology and Life Sciences
7, Kaliskiego St., 85-792 Bydgoszcz, Poland
marcinszczegielniak@poczta.onet.pl

Synthetic Aperture Sonar (SAS) is the high-resolution acoustic imaging technique which allows to improve the along-track resolution. An effectiveness of modern SAS systems strongly depends on the compensation of motion errors caused by platform path deviations. Without applying a proper processing as small deviations as a fraction of wavelength causes a serious degradation of the reconstructed SAS image. A robust motion compensation still seems to be a challenge in such a difficult environment as the restless sea. Types of motion errors, their influence on SAS systems, motion compensation methods were shortly categorized here. A few possible ways of motion compensations with their derived mathematical models are presented in the paper as well as results of numerical simulations.

INTRODUCTION

A stripmap SAS system in three-dimensional spatial domain (x, y, z) during the data acquisition is depicted in Figure 1A. The SAS system sends successive sound pulses perpendicular to the direction of the travel. In an ideal case platform's positions, at which pulses are transmitted and received, are evenly spaced on the straight platform path. The platform position and system parameters determine the size and shape of the aperture footprint on seafloor's surface. This footprint is swept along-track as the platform moves along, illuminating the swath ping by ping, so that the response of a scatterer on the seafloor is included in more than a single sonar echo. An appropriate coherent combining of the signal returns (by means of a SAS reconstruction algorithm) leads to the formation of a synthetically enlarged antenna with its length 2L (Fig. 1B), what is equivalent to obtaining high-resolution reflectivity map of acoustic backscatter strength.

The assumed the 'stop and hop' model (a platform is stationary between transmitting and receiving a signal) is not particularly valid in real conditions (it gets less precise for SAS systems operating at long target ranges) because of the low sound speed in water. However, it was assumed in order to simplify the further analysis.

1. TRANSMITTED AND RECEIVED SIGNALS

To reduce the further analysis to the two-dimensional spatial domain the new variable r called slant range was defined as

$$r = \sqrt{y^2 + h^2} \tag{1}$$

where h is the altitude of the platform and y denotes the spatial coordinate according to Figure 1A. The synthetic aperture domain will be represented by the variable $\boldsymbol{x'}$ in order to distinguish it from the x coordinate. A signal transmitted by an antenna can be written as

$$p_{tr}(t) = p(t) \cdot \exp[i\omega_c t] \tag{2}$$

where p(t) and ω_c denote **L**inear **F**requency **M**odulated (**LFM**) signal and a carrier frequency respectively.

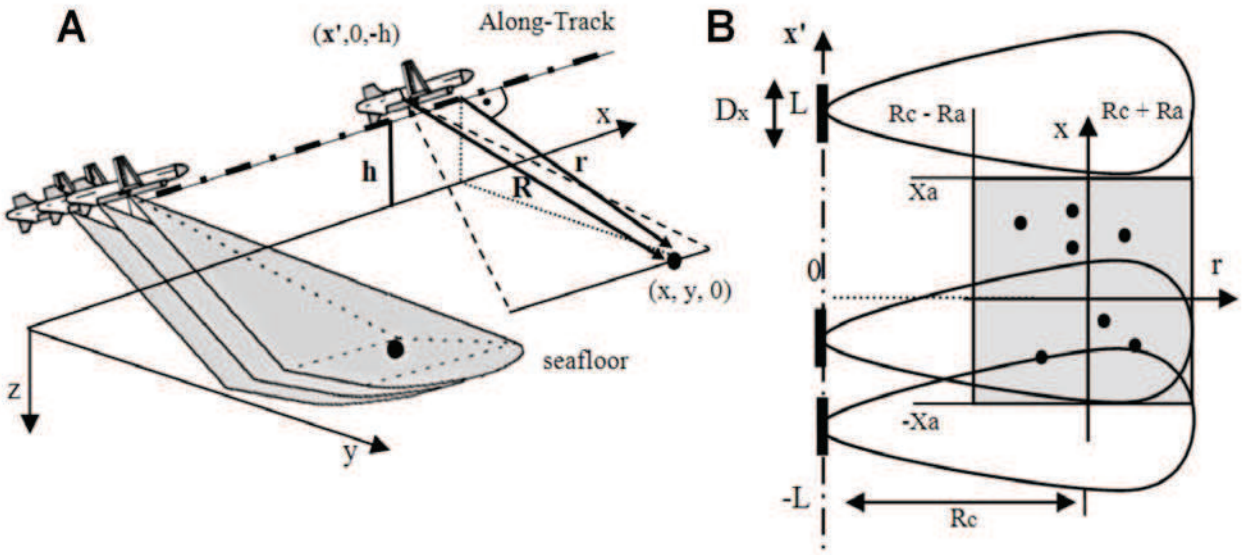

Fig. 1. Synthetic aperture imaging geometry

The received and demodulated echo signal from a scatterer located at (x,r), assuming a lossless environment and no motion errors, is then

$$ee(\boldsymbol{x'}, t) = \rho \cdot p\left(t - \frac{2\sqrt{(x - \boldsymbol{x'})^2 + r^2}}{c}\right) \cdot \exp\left[-i\omega_c \cdot \frac{2\sqrt{(x - \boldsymbol{x'})^2 + r^2}}{c}\right] \tag{3}$$

where c is the sound speed in water, ρ represents unknown reflectivity of the scatterer and $\boldsymbol{x'}$ is the position of the platform (called further simply synthetic aperture). When motion errors appears we can rewrite the equation above in the following way

$$\tilde{ee}(\boldsymbol{x}', t) = \rho \cdot p\left(t - \frac{2\sqrt{(x - \boldsymbol{x}' - X_{err}(\boldsymbol{x}'))^2 + (r - R_{err}(\boldsymbol{x}'))^2}}{c} \right) \cdot \exp\left[-i\omega_c \cdot \frac{2\sqrt{(x - \boldsymbol{x}' - X_{err}(\boldsymbol{x}'))^2 + (r - R_{err}(\boldsymbol{x}'))^2}}{c} \right] \tag{4}$$

where $X_{err}(\boldsymbol{x}')$ and $R_{err}(\boldsymbol{x}')$ are error functions in the received signal in x and r directions respectively.

2. MOTION ERRORS

A towfish can have six possible degrees of freedom in three-dimensional domain (x, y, z) as shown in Figure 2. They can be grouped in translational with three degrees of freedom (sway, surge and heave) and rotational with next three degrees of freedom (pitch, roll and yaw). It is easy to prove that the degrees of motion which affect the range dimension (yaw and sway) have a much more serious effect on the data than other degrees, especially at long ranges.

Generally, in the case of a side-looking single-transmitter and single-receiver system, sway is the main error that needs a compensation. If we extend receiver to a horizontal linear multiple receiver array, the yaw (of course, along with sway) becomes a significant factor. However, this paper deals with collocated single transmitter/receiver case. Therefore, the across-track motion error (sway) is the most important for this side-scan SAS operation [4].

On the other hand, although sway has the most effect on SAS imagery, it is the combined effect of all six degrees of freedom on the slant-range motion [5]. Mentioned above the two-dimensional mathematical model of the received SAS signal, affected by motion errors, is a representation of the three-dimensional spatial domain. If a correction of motion errors in third dimension is needed the presented model can be easily extended [2].

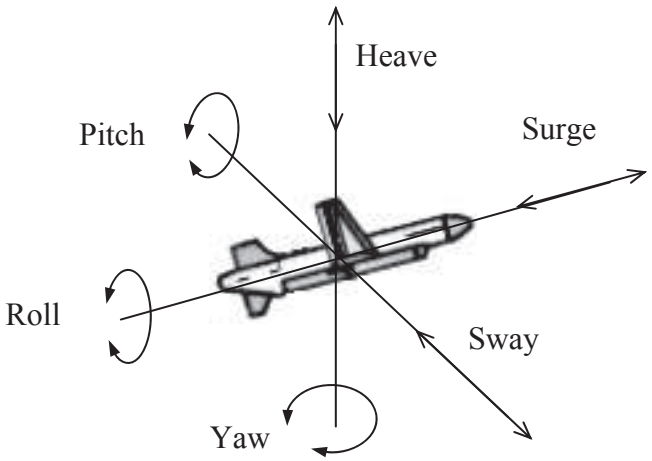

Fig. 2. Possible platform motion errors

3. POINT SPREAD FUNCTION CORRUPTED BY MOTION ERRORS

The harmful influence of the sway $R_{err}(\boldsymbol{x}')$ on SAS imaging is shown in Figure 3. The sinusoidal motion error depicted in Figure 3A was injected as a sway into platform's path and then a resultant image was obtained by means of the Omega-k reconstruction algorithm (Fig. 3B). For comparison, exactly the same error function as Xerr(x') doesn't cause any severe distortions

in point spread function (Fig. 3C). Of course, it's possible to increase the amplitude of the $X_{err}(\boldsymbol{x}')$ term in order to induce blurring or smearing of the point spread function. However, it exceeds significantly the assumed sample spacing in the synthetic aperture domain what should not be during the data acquisition and in these conditions we can simply neglect this $X_{err}(\boldsymbol{x}')$ term.

Slowly fluctuating motion errors are known to have a milder influence on SAS imaging, what can be seen in Figure 3D. Blur-free imagery requires $R_{err}(\boldsymbol{x}') < \lambda/16$ [5] and for higher order motion errors it becomes even stricter.

In practice, a yaw compensation sometimes is applied, in particular to SAS systems with an antenna array where the yaw gets more significant. Instead of performing a motion compensation which suffers from the timing error approximation (described further in the paper) for each receiver independently, it is possible to remove yaw with the use of a shift and frequency scaling of the wavenumber spectrum. However, this problem won't be analyzed here.

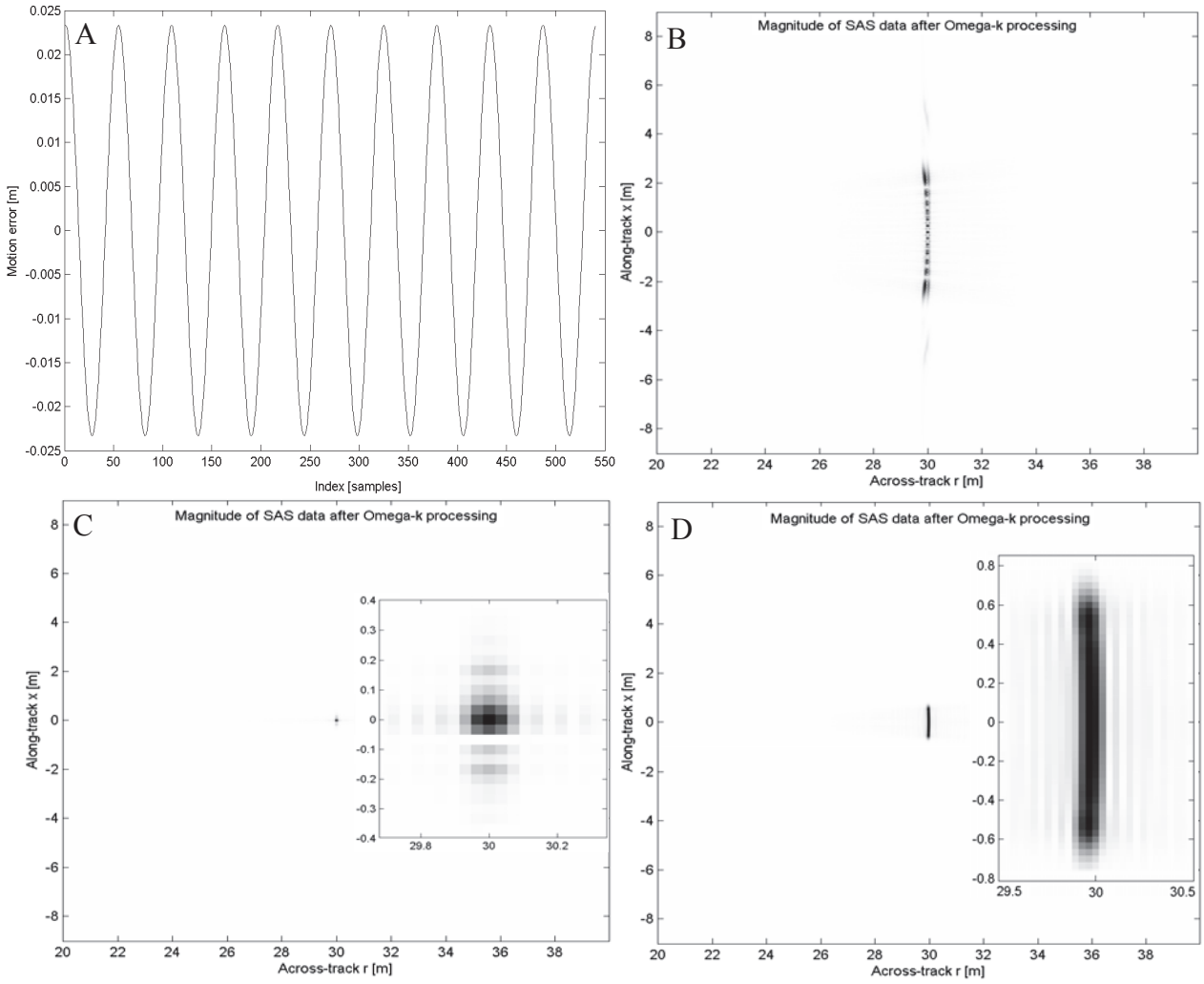

Fig. 3. Results of the numerical simulation: A) Motion errors;
B) The reconstructed SAS image of the point target with sinusoidal motion errors injected as R_{err};
C) The reconstructed SAS image of the point target with sinusoidal motion errors injected as X_{err};
D) The reconstructed SAS image of the point target with sinusoidal motion errors of four times lower frequency than 3A (injected as R_{err})

4. MOTION CORRECTION APPROACHES

Generally, there are three possible stages where motion errors can be specified. Firstly, from hardware systems during the data collection. This option seems to be the most desirable and obvious choice. But unfortunately, the accuracy of this kind of hardware systems increases with their price and usually it can't provide enough accuracy. Therefore, we have to take advantage of two next possibilities as well. We can use the raw data after data collection or the reconstructed image based on the these raw data in order to estimate and then compensate motion errors.

On the other hand, the motion compensation can be categorized according to the source of an information about motion errors. To be more precise, the motion compensation for known and unknown path errors. It is easy to guess that compensation of known path errors is possible thanks to a navigation unit (a hardware system mentioned above). The compensation for known errors can be divided into the narrow-beamwidth and wide-beamwidth in stripmap SAS systems what is discussed further in this paper.

The second group depends on estimating motion errors by means of only the collected SAS data. No *a priori* information is available here. The compensation of unknown path errors contains subaperture-based techniques often called the map drift, inverse filtering, Phase Gradient Autofocus (PGA) or Phase Curvature Autofocus (PCA) techniques and the micronavigation. The last one relies on exploiting a redundancy in the received echo data. Therefore, micronavigation requires appropriate sampling rate in the along-track direction in order to ensure the needed redundancy. In general, the micronavigation term refers to any autofocus algorithm that operates to provide a real-time estimate of the path of the travelling platform. We can rate Redundant Phase Centre (RPC) or Shear Average algorithms among this group.

The RPC technique requires the multi-hydrophone SAS array [7]. The redundant phase center technique is simply a combination of the known Vernier array concept and an idea of correlating two similar signals to estimate their relative delay. Applying single transmitter/ multiple receivers allows to estimate motion errors on the basis of received echoes by particular receivers (However, the condition of the redundancy in received data has to be met what in practice denotes overlapping the array antenna at successive platform positions).

An additional benefit of single transmitter/multiple receivers concept is a possibility of increasing the velocity of the towfish, holding required sampling rate in the along-track direction simultaneously. For a SAS array yaw errors get more dominant and should not be ignored. Therefore, SAS systems with the array antenna usually compensate sway as well as yaw errors. However, this solution will not be discussing in this paper.

PGA and PCA are a generalization of the Prominent Point Positioning (PPP) idea which will be discussed wider in the section 7.

A basic assumption of the map drift approach is that the aperture phase error function can be described by a finite polynomial expansion [6]. This method relies on dividing synthetic aperture into subapertures and then performing cross-correlation in order to estimate quadratic coefficients. The main its disadvantage is the impossibility of estimating higher order motion errors because of its parametric nature.

5. OMEGA-K RECONSTRUCTION

Let's introduce two auxiliary functions defined below

$$D_{error}(\boldsymbol{x}', x, r) = \sqrt{(x - \boldsymbol{x}' - X_{err}(\boldsymbol{x}'))^2 + (r - R_{err}(\boldsymbol{x}'))^2} \tag{5}$$

$$D_{ideal}(\boldsymbol{x}', x, r) = \sqrt{(x - \boldsymbol{x}')^2 + r^2} \tag{6}$$

which denote distances from the along-track position [$\boldsymbol{x}' + X_{err}(\boldsymbol{x}')$, $R_{err}(\boldsymbol{x}')$] affected by motion errors and the ideal one [$\boldsymbol{x}'$, 0] to a point [x, r] respectively. The Fourier transform of the received SAS data given by (4) with respect to fast-time t can be written for the entire imaged area (x, r) then as

$$\tilde{eE}(\boldsymbol{x}', \omega) = P(\omega) \iint_{xr} \rho(x,r) \cdot w_a\left[\omega, x - \boldsymbol{x}' - X_{err}(\boldsymbol{x}'), r - R_{err}(\boldsymbol{x}')\right] \cdot \exp\left[-i2k \cdot D_{error}(\boldsymbol{x}', x, r)\right] dxdr \tag{7}$$

where $k = (\omega + \omega_c)/c$ is wavenumber, term $\rho(x, r)$ describes the examined area reflectivity, $P(\omega)$ denotes the Fourier transformation of transmitted sonar signal $p(t)$ and w_a is a beam pattern of the sonar. We can rewrite the equation (7) in the following way

$$\begin{aligned} \tilde{eE}(\boldsymbol{x}', \omega) = P(\omega) \iint_{xr} & \rho(x,r) \cdot w_a\left[\omega, x - \boldsymbol{x}' - X_{err}(\boldsymbol{x}'), r - R_{err}(\boldsymbol{x}')\right] \cdot h(\omega, x - \boldsymbol{x}', r) \\ & \cdot \exp\left[-i2k \cdot D_{ideal}(\boldsymbol{x}', x, r)\right] dxdr \end{aligned} \tag{8}$$

where $h(\omega, x - \boldsymbol{x}', r) = \exp\left[i2k \cdot \Delta D(\boldsymbol{x}', x, r)\right]$

$$\Delta D(\boldsymbol{x}', x, r) = D_{ideal}(\boldsymbol{x}', x, r) - D_{error}(\boldsymbol{x}', x, r)$$

If we treat the equation (8) as **AM-PM** (**A**mplitude-**M**odulated-**P**hase-**M**odulated) signal [2], where $w_a(\cdot)$ and $h(\cdot)$ are slowly fluctuating **AM** components in comparison with **PM** component $\exp\left[-i2k \cdot D_{ideal}(\boldsymbol{x}', x, r)\right]$, we can determine this signal in ($k_{x'}$, ω) domain using the known method of stationary phase. Then we have

$$\tilde{EE}(k_{x'}, \omega) = P(\omega) \iint_{xr} \rho(x,r) \cdot W_a(\omega, k_{x'}) \cdot H(\omega, k_{x'}) \cdot \exp[-ir \cdot \sqrt{(2k)^2 - (k_{x'})^2} - ix \cdot k_{x'}]\, dxdr \tag{9}$$

where $H(\omega, k_{x'})$ is the simple scaling form of the term $h(\omega, x - \boldsymbol{x}', r)$ defined in the following way

$$H\left(\omega, 2k \frac{x}{\sqrt{x^2 + r^2}}\right) = h(\omega, x, r) \tag{10}$$

or

$$H(\omega, 2k \sin\theta(x')) = h(\omega, x - x', r) \tag{11}$$

where $\theta(\boldsymbol{x}')$ is the aspect angle of the sonar for the target (x, r) when the sonar is located at [$\boldsymbol{x}' + X_{err}(\boldsymbol{x}')$, $R_{err}(\boldsymbol{x}')$]. The same relationship concerns the amplitude beam pattern $W_a(\cdot)$.

The Omega-k reconstruction algorithm relies on the Stolt mapping defined below

$$k_r = \sqrt{k^2 - k^2_{x'}} \tag{12}$$

$$k_x = k_{x'} \tag{13}$$

Applying Slolt mapping to (9), we get

$$\widetilde{EE}(k_x,k_r) = P(\omega)\iint_{xr} \rho(x,r)\cdot W_a(\omega,k_x)\cdot H(\omega,k_x)\cdot \exp[-ir\cdot k_r - ix\cdot k_x\ ]dxdr \tag{14}$$

From motion compensation's point of view the most important are equations (10, 11) and (12, 13). With the aid of them we can reveal the following mapping from (k_x, k_r) to ($\boldsymbol{x'}$, ω) domain

$$H(k_r,k_x) = h(\omega, x-\boldsymbol{x'}, r) = \exp[i2k\cdot \Delta D(\boldsymbol{x'},x,r)] \tag{15}$$

$$2k = \sqrt{k_r^{\,2} + k_x^{\,2}} \tag{16}$$

$$\boldsymbol{x'} = x - \frac{k_x}{k_r} r \tag{17}$$

To recap, an ideal SAS signal $EE(k_x,k_r)$ can be related to $\widetilde{EE}(k_x,k_r)$ corrupted one by motion errors

$$\widetilde{EE}(k_x,k_r) = EE(k_x,k_r)\cdot \exp\left[i\sqrt{k_r^{\,2} + k_x^{\,2}}\cdot \Delta D(x-\frac{k_x}{k_r}r, x, r)\right] \tag{18}$$

$H(k_r,k_x)$ can be considered as the spatially varying filter then. The reconstructed SAS image, which should to estimate the desirable function $\sigma(x,r)$, corrupted by motion errors is

$$\widetilde{\rho}(x,r) = \iint_{kx\,kr} \widetilde{EE}(k_x,k_r)\cdot P^*(\omega)\exp[ik_r\cdot R_c]]\cdot \exp[ik_r\cdot r + ik_x\cdot x]dk_x dk_r \tag{19}$$

where $P^*(\omega)$ is the complex conjugate of $P(\omega)$.

The additional term which has appeared in the above equation allows to bring this signal to the lowpass, i.e. this operation lets us to center the resultant SAS image at the reference distance R_c. According to Fig. 1B, R_c and X_c represent the center of the illuminated area in the across-track and along-track domain respectively. The described case is a broadside type, where $X_c=0$. If it is not, we should introduce the additional function in the form $\exp(ik_xX_c)$.

6. MOTION COMPENSATION FOR KNOWN MOTION ERRORS

A navigation unit can be used to obtain an estimate of motion errors [$X_{err}(\boldsymbol{x'})$, $R_{err}(\boldsymbol{x'})$]. On the basis of this information, we can remove known motion errors, and thus blurring in the final SAS image. The simplest way assumes narrow beamwidth of the sonar what results in neglecting space-variant nature of the $\Delta D(\boldsymbol{x'},x,r)$ function. It's possible thanks to the following approximation

$$\Delta D(\boldsymbol{x'},x,r) \approx R_{err}(\boldsymbol{x'}) \tag{20}$$

There is no need to perform the motion compensation by spatially varying filter (according to the equation (18)), because the approximation above makes the filter $H(k_r, k_x)$ space-invariant. So, we can remove motion errors from pulse-compressed SAS data in ($\boldsymbol{x}'$, ω) domain by the simple operation

$$eE(\boldsymbol{x}', \omega) = \tilde{eE}(\boldsymbol{x}', \omega) \cdot \exp\left[-i2kR_{err}(\boldsymbol{x}')\right] \tag{21}$$

This solution is often called timing-error approximation. Narrow-beamwidth compensation assumes that a sideways displacement from the straight flight-path can be treated as an equivalent timing-error in the raw SAS data

$$ee(\boldsymbol{x}', t) = \tilde{ee}\left(\boldsymbol{x}', t - \frac{2R_{err}(\boldsymbol{x}')}{c}\right) \tag{22}$$

For a wider beamwidth this model gets less precise. If the timing-error approximation is not acceptable we should apply wide-beamwidth model according to (18), i.e.

$$EE(k_x, k_r) = \tilde{EE}(k_x, k_r) \cdot H^*(k_x, k_r) \tag{23}$$

where $$H^*(k_x, k_r) = \exp\left[-i\sqrt{k_r^2 + k_x^2} \cdot \Delta D(x - \frac{k_x}{k_r} r, x, r)\right]$$

The filtered out single point $\tilde{\rho}(x, r)$ in the resultant SAS image with compensated motion errors is obtained by applying the filter $H^*(k_r, k_x)$ for that point and then performing inverse Fourier transform.

The problem connected with the model based on the Fourier property of **AM-PM** signals (derived in the previous section) is that the AM component ought to be slowly fluctuated one. It is highly probable that we will have to deal with higher order phase errors in practical wide-beam SAS systems. One way of mitigating this problem [2] is to perform the narrow-beamwidth compensation, and then apply the wide-beamwidth compensation with the new filter

$$H^*(k_x, k_r) = \exp\left[-i\sqrt{k_r^2 + k_x^2} \cdot \Delta D_{\boldsymbol{modified}}(x - \frac{k_x}{k_r} r, x, r)\right] \tag{24}$$

where $$\Delta D_{\boldsymbol{modified}}(\boldsymbol{x}', x, r) = \Delta D(\boldsymbol{x}', x, r) - R_{err}(\boldsymbol{x}')$$

Narrow-beamwitdh compensation allows to reduce the fluctuations and dynamic of the $h(\omega, x - \boldsymbol{x}', r)$ term and thus makes the derived model more accurate.

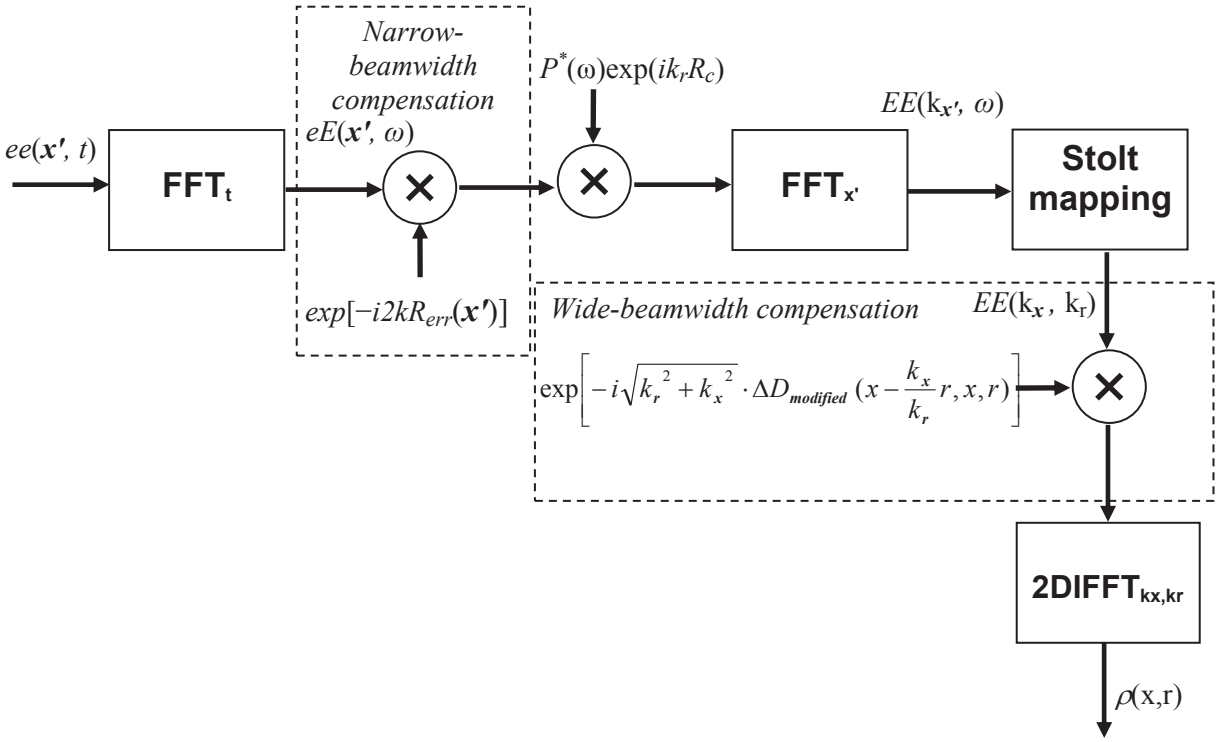

Fig. 4. The two-stage motion compensation scenario

7. INVERSE FILTERING

Inverse filtering is an autofocus technique which is often called Prominent Point Positioning (PPP). It assumes that it is possible to remove motion errors, and thus the harmful blurring, on the basis of the information contained only in the reconstructed SAS image. Let's recall the narrow-beamwidth approximation given by the equation (20). Our filter can be written then in the fallowing way

$$H(k_x, k_r) \approx \exp[i2kR_{err}(x')] \tag{25}$$

or more general, for a squint narrow-beamwidth SAS system

$$H(k_x, k_r) \approx \exp[i2kR_{err}(x')\cos\theta_S + i2kX_{err}(x')\sin\theta_S] \tag{26}$$

where θ_S is the squint angle. We stated earlier that this filter can be used for the motion compensation of known path errors. It's possible to estimate such the filter by means of a prominent target (x_p, r_p) in the reconstructed SAS image as well. All we have to do is to extract the SAS image signature $h(x - x_p, r - r_p)$ of this target. Performing the inverse Fourier transform we get

$$H(k_x, k_r) \approx \exp[i2kR_{err}(x')]\exp[ik_x x_p + ik_r x_p] \tag{27}$$

Next, we should remove the linear phase connected with the position of the prominent point target in the reconstructed SAS image. Otherwise, the motion correction would cause the shift of all targets. The final motion compensation is done by

$$F(k_x, k_r) \approx \widetilde{F}(k_x, k_r) \cdot H^*(k_x, k_r) \tag{28}$$

8. CONCLUSIONS AND REMARKS

The mathematical model was derived for the Omega-k reconstruction, taking into account motion errors, narrow-beamwidth and wide-beamwidth motion compensations as well as the autofocus method called inverse filtering.

Then numerical simulations of a SAS system in the stripmap mode were executed in the Matlab environment (assumed parameters of simulations were listed in Table 1). A received raw stripmap SAS data affected by the destructive sway error were generated (Figure 5B). The sway error injected into this received SAS signal is shown in Figure 5A. Next, the two-step motion compensation scenario (narrow-beamwidth and wide-beamwidth, according to the diagram in Figure 4) for this known sway error (for example, delivered by a navigation unit) with the use of the Omega-k reconstruction was applied. The result of this processing is depicted in Figure 5D. Comparing this reconstructed image with Figure 5C (where only narrow-beamwidth compensation was applied), it is easy to note that the two-stage compensation scenario is more effective (particular point spread functions are better focused).

The executed numerical simulations confirmed the advantage of the two-step scenario in the compensation of the sway error over only narrow-beamwidth compensation.

In the second simulation the inverse filtering method was applied in order to enhance the reconstructed and corrupted SAS image (Fig. 6A). The sway error injected into the received SAS signal is shown in Figure 6C. Please, note. The amplitude of this sway is a lot less than in the last case (about thousand times less than in the Figure 5A). Looking at the reconstructed image we can observe how vulnerable a SAS system is on motion errors. Deviations of the path as small as a few millimeters cause a visible degradation and blurring the point spread functions in along-track direction. Of course, it decreases an actual resolution of this kind of systems.

Inverse filtering technique was used here in order to estimate motion errors on the basis of the reconstructed SAS image (6A) and then using this estimation to correct the SAS image. To be more precise, the filter described in the section 7 was derived for only one prominent point (selected in the Figure 6A). After the applying this filter according to the equation (28) and the Inverse Fourier Transform we get the corrected SAS image shown in Figure 6B.

We can note that all point targets at the same along-track coordinate as the chosen prominent point are corrected properly. However, the point slightly distant from the prominent target in along-track direction suffers from the severe blurring. This is because of a space-variant nature of the SAS data in the stripmap mode. To be more precise, the problem is that targets at different along-track positions in the imaging scene 'see' the shifted error function $R_{err}(\boldsymbol{x'})$.

One could assume range-invariant blurring and find a prominent point at every along-track line in order to remove motion errors from the entire SAS image this way.

Table 1. Assumed parameters of the simulation

c (sound speed in water)	1500 [m/s]
Chirp bandwidth	5 [kHz]
Chirp duration	5 [ms]
Carrier frequency	100 [kHz]
Dx (sonar diameter in the along-track direction)	0.16 [m]
Across-track resolution	0.0750 [m]
Along-track resolution	0.0800 [m]
2*Ra (examined seafloor in the range direction)	20 [m]
2*Xa (examined seafloor in the azimuth direction)	10 [m]
Rc (distance to the center of the examined area)	30 [m]

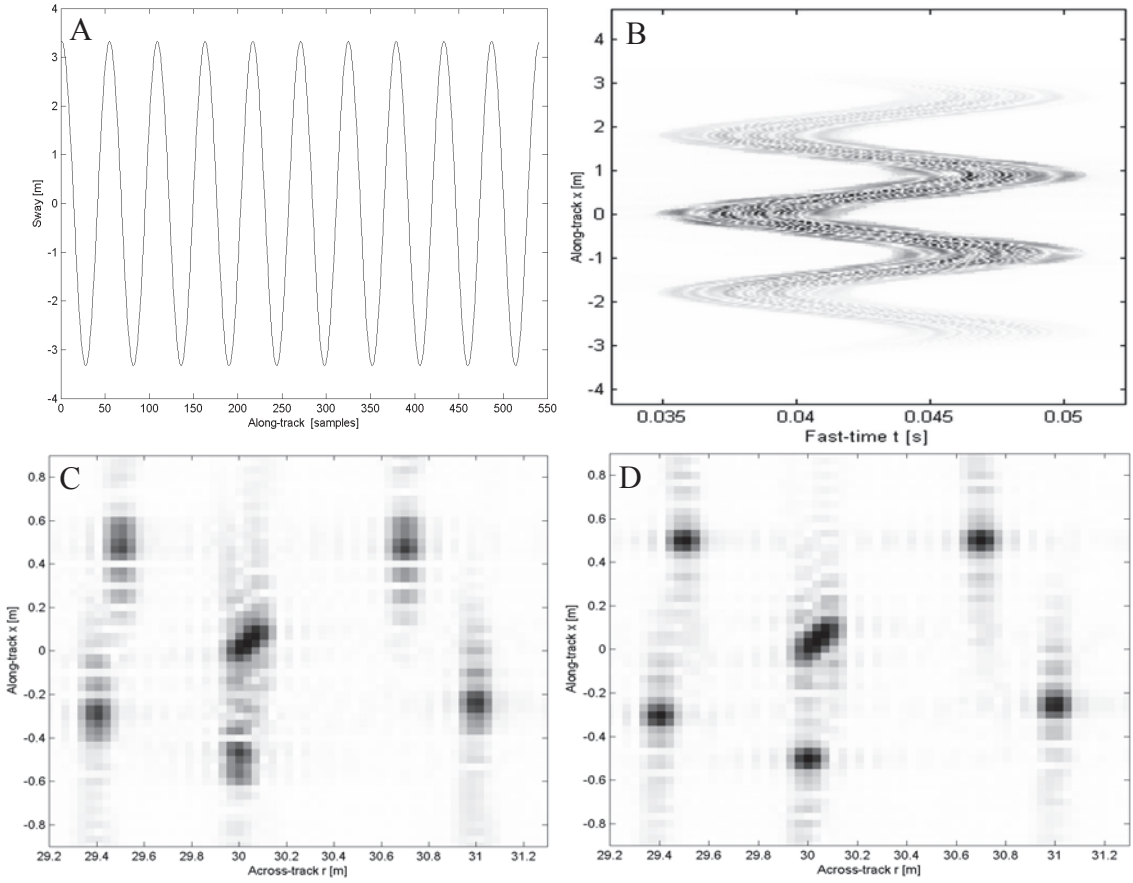

Fig. 5. Results of numerical simulations: A) Motion errors injected into the received SAS data; B) Received the raw SAS data; C) The reconstructed SAS image after narrow-beamwidth motion compensation; D) The reconstructed SAS image after narrow-beamwidth and then the modified wide-beamwidth motion compensation

Unfortunately, it doesn't seem to be a practical case. There are not particularly many prominent targets in real received SAS signals. Moreover, these targets should be well-isolated from other surrounding targets. There are more efficient algorithms such as PCA or SPGA [5] which take advantage of a redundancy of the phase error function. However, the idea is very similar.

A robust motion compensation still seems to be quite difficult task in practical stripmap SAS systems. Especially, the performance of autofocus algorithms highly depends on the imaging scene and the nature of motion errors.

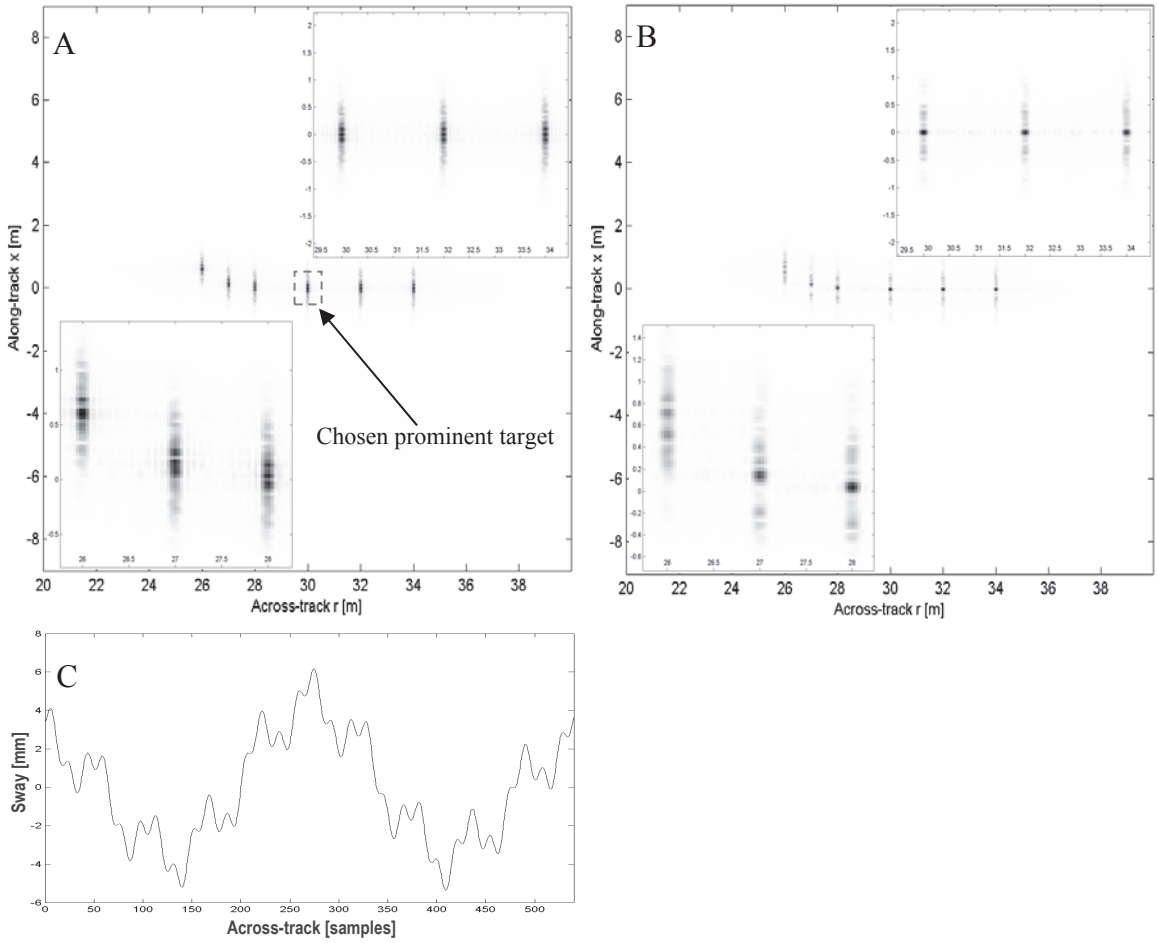

Fig. 6. Results of numerical simulations: A) The reconstructed SAS image with the presence of motion errors; B) The reconstructed SAS image after inverse filtering; C) The injected sway

REFERENCES

[1] Bonifant W., Interferometic Synthetic Aperture Sonar Processing, MSc thesis, Georgia Institute of Technology, 1999, 38–39.

[2] Soumekh M., Synthetic Aperture Radar Signal Processing, John Wiley & Sons, USA, 1999, 226–230, 223–226.

[3] Szczegielniak M., Przetwarzanie danych SAS przy pomocy algorytmu Omega-K, Otwarte Seminarium z Akustyki, Poznań – Wągrowiec 2005.

[4] Hayes M. P., Gough P. T., Broad-Band Synthetic Aperture Sonar, IEEE Journal of Oceanic Engineering, Jan. 1992, 80–94.

[5] Callow H. J., Signal Processing For Synthetic Aperture Sonar Image Enhancement, PhD thesis, 6, 79, 153, Electrical and Electronic Engineering at the University of Canterbury, New Zealand 2003.

[6] Jakowatz C. V., Wahl D. E., Spotlight-Mode Synthetic Aperture Radar: A Signal Processing Approach, Springer 1996, p. 245.

[7] Gough P. T., Miller M. A., Displaced Ping Imaging Autofocus For A Multi-Hydrophone SAS, IEE Proc.-Radar Sonar Navig., Vol. 151, No 3, June 2004.

[8] Heremans R., Dupont Y., Acheroy M., Motion Compensation In High Resolution Synthetic Aperture Sonar (SAS) Images, Advances in Sonar Technology, Sergio Rui Silva (ed.), I-Tech Education and Publishing, 2009.